Journal of Intelligent Manufacturing
https://doi.org/10.1007/s10845-022-01991-4

Automated manufacturability analysis in smart manufacturing systems: a signature mapping method for product-centered digital twins

Kaishu Xia[1] · **Thorsten Wuest**[2] · **Ramy Harik**[1]

Received: 22 June 2021 / Accepted: 6 July 2022

Abstract
Developing affordable and customizable cyber-physical production system and Digital Twin (DT) implementations infuses new vitality for current Industry 4.0 and Smart Manufacturing initiatives. The ability to precisely address material handling processes for manufacturability analysis further connects the physical and cyber components of today's smart manufacturing systems. In this work, we propose a product-centered signature mapping approach to automated digital twinning featuring a hybrid implementation of smart sensing, signature-based feature extractor, and knowledge taxonomy. First, we integrate 3D scanning and surface reconstruction at to implement shape retrieval from both the virtual environment (from Computer-Aided Engineering data) and the real-world production environment (from scanned point cloud frames). Second, *Shape Terra*, an algorithm for intrinsic curvatures, simulates Persistent Heat Values for fast signature extraction from retrieved shape files. Finally, a systematic integration of the proposed shape analysis based on knowledge taxonomy is prototypically implemented. The objective of this testbed is to illustrate a proof-of-concept DT-aided process autonomy fed by rapid 3D surface signatures. As a result, by hybridizing smart sensing and simulative approaches, we exploit shape signatures as manufacturing knowledge by integrating domain knowledge and data-driven decision-makings. Moreover, human–machine interoperability enabling system-level intelligent controls becomes feasible in complex material handling, shape forming, measuring, and inspection processes.

Keywords Smart manufacturing systems · Semantic interoperability · Feature extraction · Digital twin · Manufacturability analysis

Introduction

Rapid advances in collaborative computing entities that tightly connect physical world and its ongoing processes, have inspired networked devices to sense, monitor and actuate physical elements. Such system-embedded devices are considered the root of cyber-physical systems (CPS) (Monostori et al., 2016). Industrial cyber-physical production systems (CPPSs) connect manufacturing physical and cyber components at system-level and thus facilitate simultaneous process optimization and efficient human–machine interoperability to further exploit manufacturing science and technologies beyond computing, information and communication benefiting from CPS architectures. Advancing CPPSs towards standardized and generally acceptable manufacturing paradigms is at the heart of current smart manufacturing innovations leading to Industry 4.0 (Monostori et al., 2016). To that end, real-time sensing and information fusion are expected to couple digital tools with physical manufacturing assets, including entities, processes, assets, and products. Identifying which process data should be captured, analysed, and shared is essential for manufacturers to maximize their products' add-on values. Hence, enabling customizable knowledge streams for cyber-physical production systems (CPPS) and Digital Twins (DTs) implementations infuses new vitality for current Industry 4.0 and Smart Manufacturing initiatives.

✉ Ramy Harik
harik@mailbox.sc.edu

[1] Department of Mechanical Engineering, University of South Carolina, Columbia, SC 29201, USA

[2] Department of Industrial and Management Systems Engineering, West Virginia University, Morgantown, WV 26506, USA

Published online: 06 August 2022

Conceptually similar to 3C (Computation–Communication–Control) components of CPSs, cognitive DTs have developed various manufacturing applications by exploiting implicit knowledge from legacy production systems. For examples, standardization of data schema in cloud-based digital manufacturing systems (Park et al., 2020), enabling automated dataflow models to reflect real-time progress measurements (Ebel et al., 2021), building reference architectures to exchange information between connected entities (Redelinghuys et al., 2020), advancing information extraction techniques such as query-based graph learning (Mortlock et al., 2021), connecting and interoperating between product twins, process twins, and operations twins for closed-loop, real-time interactions (Bao et al., 2019), applying a D-M-S (Data, Model, and Service) framework to conventional IoT systems to realize collaborative framework between the edge and cloud (Jiang et al., 2021). Compared to CPS's core topics on system components, DT focuses on acquired data and their model's capability to manage physical production entities (Tao et al., 2019). One challenge for manufacturers is to develop adaptive process planning using reliable and affordable knowledge systems. For instance, inherent and recallable information used to identify product features, or other genetically intelligent properties (Denkena et al., 2010), such as geometry and topology, can be stored as static data and reflect product inherent properties. It can be envisioned that geometrical and topological studies of product structures in production are nonnegligible modelling approach to increase understandings of processes involving material handling, shape forming, measurement and quality inspection. DTs to retrieve run-time 3D information in point clouds and meshes is a yet-to-accomplished task for most legacy manufacturing systems.

Feature-based technologies have been extend to smart design/engineering in DT systems (Schleich et al., 2017), adaptive process control (Adamson et al., 2017), augmented reality (Lai et al., 2020), Artificial Intelligence (AI) enabled process planning (Marchetta & Forradellas, 2010), etc. Shape-critical patterns are extracted from topological and geometrical data and form representational schemes of manufacturing features. Extracted feature representation are widely used for the downstream process planning and optimization applications. For instance, in Computer-Aided Manufacturing (CAM), the algorithms to identify product shape features have significantly contributed to the automated planning for material handling processes, typically shape-forming or material-removing procedures such as CNC. To name a few, processes involving the configuration of work piece holding (Rameshbabu & Shunmugam, 2009), choice of machines and cutting tools (Zhang et al., 2014), or planning of the machining operations (Geng et al., 2016). Usage of data mining, machine learning, or AI for shape feature recognition have been rapidly evolving, given the well-developed computation technologies to handle large volumes of complex, noisy, high-dimensional, and unorganized datasets, such as point cloud and surface meshes. However, they usually require abundant training datasets with meaningful and balanced distribution of features, which can be expensive to collect in many industrial settings.

Several recent applications of smart sensing have been discussed to enhance legacy production processes, such as using visual inputs to in-situ automated inspection (Davtalab et al. 2020) (Li et al., 2021). Manual 3D modelling and measurement are aided by in-situ visual sensing and 3D reconstruction (Zhang et al., 2013). Visual sensing has been tailored to production use cases, such as automated inspection and cutting tool monitoring. However, precision of reconstruction, measurement, and defect detection using images can be compromised without adequate data utilization. Moreover, there have been few studies on 3D surface quality based on point cloud data or surface retrieval (Zhao et al., 2021) given the difficulty of runtime data to generate high resolution intelligence to physical shop floors as value-adding production processes. The real-time requirement of critical tasks such as in-situ product visual inspection will not be ready without systematic reliability in current Smart Manufacturing Systems (SMSs). As new visual-depth sensors becoming more and more integrated into production, rapid non-contact technologies are to be developed to handle these temporal, high dimensional, noisy, and expensive inputs. For instance, Non-uniform rational basis spline (NURBS) surface input to conventional Statistical Process Control (SPC) was evaluated in (Wells et al., 2013) (Wells et al., 2021) by converting complex surfaces into linear profiles. This work monitors deviation from expected nominals and failure modes as benchmark and extract control variables. (Zhao et al., 2021) applies surface segmentation and classification using machine/deep learning. This approach introduces explicit steps to utilize Principle Component Analysis (PCA) for dimensional reduction, and then learns to segment and classify classified regions. Similar data-driven techniques need to be carefully designed to utilize high-fidelity raw stream without losing local information. Such learning-based methods also require abundancy, balancing, and quality of training datasets, which may be expensive for many part inspection and measurement tasks. Learning-based methods could further induce model complexity and require expert knowledge for proper usage, such as manual definition of regions numbers, which are demanding knowledges for industrial practitioners. Assisting by CAD data, on-machine tool path generation based on point cloud registration is explored in (Huang et al., 2021). This work is demonstrated to generate accurate path by hybrid modelling. Accurate alignment between CAD and point cloud is through knowledges such as calibrated transformation matrix, which can be changeable, expensive, or unavailable. In summary,

reliable 3D shape retrieval tasks enabled by technologies such as multi-modal learning (Nie et al., 2020) has not demonstrated their readiness in today's production systems. Data correlation and consistency evaluation approaches need to be developed for comparison among industry applicable datasets (Zhang et al., 2020).

In this work, we propose a shape signature-based approach to digital twinning that addresses the problem of precisely sensing material handling processes for manufacturability analysis. This paper first investigates the approach of extracting shape signatures and its pattern recognition method, namely the heat kernel signatures. To fill the current knowledge gaps between CAD shapes and scanned shapes, as well as expand the usage of feature recognition, the authors then propose to utilize simulative geometrical analysis coupled with 3D sensing. This combination facilitates rapid detection process of structural variances with perturbation from environmental changes and production activities. Finally, a signature mapping mechanism with a shape search enabled by comparison is outlined to demonstrate in-situ shape knowledge retrieval for automated manufacturing use cases.

The remainder of this paper is structured as follows: *Related Work* introduces the scientific background of the heat-based signature models. *Methods and Research Materials* proposes a D-M-S procedure for system implementation of digital twinning. *Results and Discussion* presents the results with respect to the persistence clustering, multiscale filtering, shape mapping, and signature pool establishment, and knowledge integration. *Conclusion and Outlook* concludes the paper, briefly highlights the contribution and summary of the presented research, finally provides an outlook on future work.

Related work

Knowledge-based engineering (KBE) applications facilitate various information streams, information structures and knowledge modelling templates for CAD/CAE (Pokojski et al., 2021). Sharing of knowledge demonstrates its importance in today's multi-process, multi-intersection, and multi-operator subsystems towards collaborative efforts between designing, manufacturing, and supply chains (Zhang & Ming, 2020). By utilizing an improved representation model of user requirement, the details of production can be further improved in the forms of reduced production time, cost, process accuracy, and finally the delivery committed rate (Xia et al., 2021a, 2021b). However, the up-to-date reference architecture models are found to be lack of compatibility and interoperability while the communication and information technologies are ready for such standardization (Yli-Ojanperä et al., 2019).

Manufacturing features have been widely used for manufacturability analysis and downstream process planning activities such as the configuration of work piece holdings, choice of manufacturing machines and cutting tools, and planning of the machining operations. For instance, automated machining process planning using CAPP software is started by classifying CAD geometrical features using historical databases, followed by identifying feasible machine sequences (Liu et al., 2015) (Nonaka et al., Generating alternative process plans for complex parts, 2013). Staring from model features and available resources, shop-floor operation optimization can be further achieved by looking into alternative plans with a minimization of setup and operational time and perform adaptive scheduling (Nonaka et al., 2012). Depending on the applications and input models, feature recognition techniques using representations such as face adjacency graphs, convex hull, volumes, and cells have been successfully developed (Shi et al., 2020a, 2020b). These majority of these feature representations based on CAD and/or CAM data which are created with well-defined topological and geometrical elements. In more challenging cases, freeform surfaces with arbitrary face interactions or curvatures (Sundararajan & Wright, 2004) require additional assumptions (Dong & Vijayan, 1997), recognition rules (Sunil & Pande, 2008), mathematical modelling (Belkin et al., 2008), segmentation or classification methods (Cai et al., 2018).

This work intends to implement a novel approach to the geometrical analysis of rapidly 3D scanned surfaces. The feature extraction is performed based on *Shape Terra* (Harik et al., 2017). *Shape Terra* has been successfully applied to provide accurate manufacturability analysis (Shi et al., 2018) and feature recognition by an convolution neural network approach (Shi, Zhang, & Harik, Manufacturing feature recognition with a 2D convolutional neural network, 2020) on CAD datasets. This section will explain the novelty of heat-based shape signatures used in 3D scan data.

To quantify freeform surfaces, natural geometric properties (such as intrinsic curvatures) in Euclidean domains and Riemannian manifolds were mathematically estimated using heat kernels and the eigenfunctions of Laplacian (Jones et al., 2008). Constraining the heat kernels on a temporal domain further defines the pointwise Heat Kernel Signatures (HKS) by (Sun et al., 2009). HKS propose a shape signature that is invariant to isometric transformation, which enables the geometrical comparison of different shapes and meshes. In addition, HKS has proven to be informative, multi-scale, stable under perturbation, and commensurable. One unresolved problem of HKS is the sensitivity to shape scaling, which can be solved by applying a Fourier transformation (Bronstein & Kokkinos, 2010). This is inspired by scale invariance on images (Kokkinos & Yuille, 2008). Based on multi-scale property of HKS, a multi-resolution approach as faster shape

manipulation algorithm (*fast HKS*) is proposed (Vaxman et al., 2010) by restricting to different resolution level. This overcomes the limitation of computational complexity and modest mesh resolutions. A concept of Persistent Heat Signature (Dey et al., 2010) is proposed to solve the pose-oblivious matching of incomplete models from partial scanning. Persistent Heat Signature extracts a feature vector composed of the HKS maxima and uses it to search for most similar complete, partial, or incomplete models in a database. Coupled with PCA and clustering, Heat Kernels have also been successfully applied to characterizing the topological structure of individual graph in large collections of graphs (Bai et al., 2005). Heat Kernel embedding is furtherly developed as a representation of differential geometries and graph structures by mapping of the nodes of a graph into a vector-space (ElGhawalby & Hancock, 2015).

The use of heat kernels is also expanded to the problem of nonrigid shape retrieval in large databases (Bronstein et al., 2011) by using multiscale diffusion heat kernels as "geometric words" and creating spatially sensitive bags of features with better discriminative power within big datasets. This work also shows that shapes can be efficiently represented as binary codes to ensure a machine-readable and searchable format.

Shape Terra (Harik et al., 2017) proposed an approach to address CAD shape recognition problems by simulating the effect of the shape characteristics to its heat retention time. Using this approach, a unique shape signature is created for each point, which inherits the properties of HKS (Sun et al., 2009). Through the calculation of heat losses, the persistence of a point to retain heat and its resistance to heat loss can be used to calculate retention levels and values. Similar persistence values can then be clustered, and these are filtered to segment clusters containing manufacturing features. The features can then be compared with isolated features to further classify. As a use case scenario, features obtained from the 3D scans can be numerically compared with ones extracted from a CAD mesh file.

Inherited from HKS property of multiscale matching and invariance under isometric transformation, heat persistence can be used as the shape recognizer to differentiate pose-oblivious shapes by comparing their signatures (Dey et al., 2010). This enables the identification of intrinsic geometries from different structures, to quantitively distinguish surface dimensions, quality, and surface defects.

Methods and research materials

This section will introduce the acquisition of the shape data within a virtual-physical production system via two pipelines: CAD shape data that is retrieved from virtual environment; and surface shapes retrieved from 3D scanning device in a real-word manufacturing cell. Data is collected from a highly automated robot assembly cell enabled by CPS infrastructure featuring AI (Xia et al., 2020) and smart sensing (Saidy et al., 2020). The roadmap to integrate signature-based knowledge into legacy production system by Data-Model-Service (D-M-S) approach is summarized. The research activities are then conducted in a Data-Model-Service (D-M-S): approach: (1) Data collection and preprocessing. At this stage, shape mesh files are acquired structures from virtual models, point cloud, or reverse engineering by structural reconstruction, etc., and data scrubbing to formulate consistent inputs for *Shape Terra*. (2) Simulate *Shape Terra* on manufactured products on denoised surfaces with significant feature patterns for extraction. Depending on the specific datasets and needs, feature recognition can be performed by both rule-based systems and statistical methods such as machine learning. (3) Knowledge deployment. At the final stage, knowledge derived semantically from *Shape Terra* is integrated into CAE platform and control systems.

D-M-S to digital twinning

Figure 1 shows systematic approach to proposed product-centered, signature(feature)-based Digital Twin using a Data-Model-Service (D-M-S) framework. System development using a D-M-S approach to Digital Twinning, integrates 3 steps for a product-centered manufacturing digital twin:

- Data (D): Automated region segmentation and feature extraction from raw data in forms of 3D scans or CAD files at the first step. Heat Signatures and clustering are calculated and matched for semantic features for file individuals.
- Model (M): Depending on the manufacturing processes, engineering knowledge will be input to generate feature-level insights during the design and manufacturing phases. Meanwhile, feedback extracted from the raw data will continuously improve design/manufacturing entities.
- Service (S): To increase the efficiency, adaptiveness and agility of designers, manufacturers, and supply chains, information flow and feedback from different phrases (rule or requirement-based engineering, production processes, supply or demand, etc.) will be input towards such as a make or buy decision recommended by manufacturability analysis.

Values from high-dimensional and temporal production data are added to current digital twin system with the potential to provide closed-loop improvement to designers, manufacturers, supply chains, and decision makers. Compared to recent DT and knowledge-based engineering implementations (Mortlock et al., 2021) (Jiang et al., 2021) (Redelinghuys et al., 2020) (Pokojski et al., 2021), this work

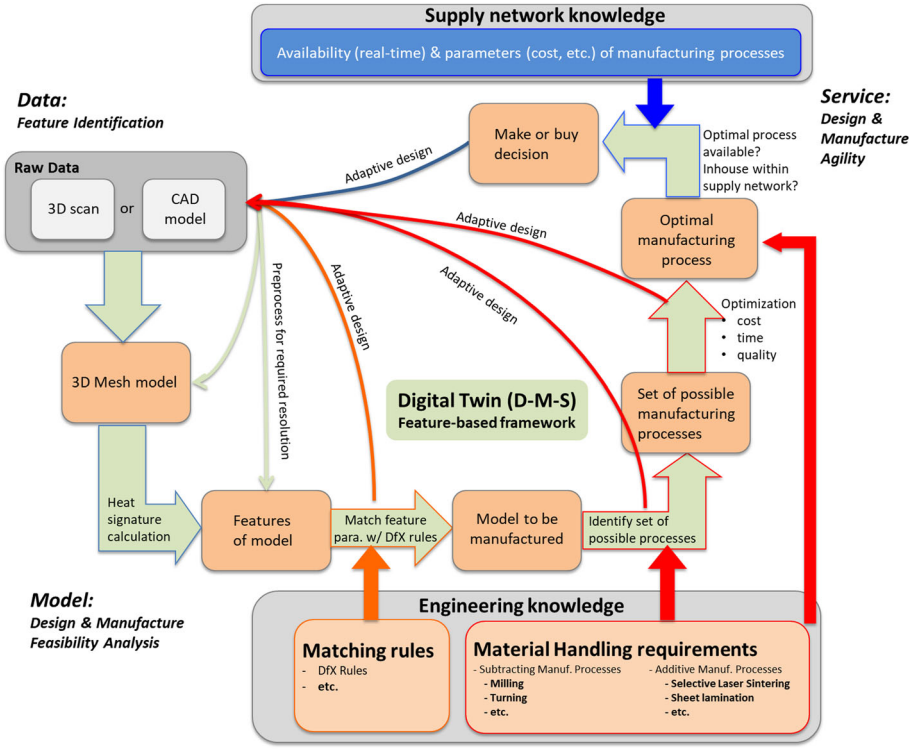

Fig. 1 Data-model-service framework to proposed product-centered, signature(feature)-based digital twin

intends to prepare for run-time high-resolution data value added to legacy production systems. Frame-wise depth image with depth can be semantically segmented, extracted, and mapped to manufacturing features using heat signature calculation deployable to computing devices. Based on specific use cases, human–machine interoperability can be designed by either manually querying established knowledge base or automated applications such as machine learning. By which means, collaborative manufacture is further enhanced by connected entities with increased agility enhanced by digital twinning at higher resolution.

Data acquisition

The experimental factory setup is demonstrated in Fig. 2. Cameras with depth sensors are mounted along the conveyor and on the robot end effect to monitor the process, product, and material flow. In this work, we use Intel® RealSense™ LIDAR L515 RGB-D cameras to scan 3D printing parts. Incoming parts are scanned within a raw manufacturing scene with registered depth information. Process control decisions can be made based on the inference results of proposed system-level digital twin (Xia et al., 2020). RGB images machine visual recognition using deep learning approach has been designed to monitor the process including the interactions or relative position among the equipment, parts, and markers (Xia et al., 2021a, 2021b). State-of-art point cloud processing and recognition algorithms in machine learning field can solve tasks of object classification, detection and semantic segmentation, such as VoxelNet (Zhou & Tuzel, 2018) and PointNet (Charles et al., 2017). Learning-based system for real-time mapping in in-door scenes scanned by depth camera is achieved at large scales (Newcombe et al., 2011). Object detection through trained machine vision network on RGB frames (Xia et al., 2021a, 2021b) can also automatically crop RGBD frames. Proposed digital twin system framework is shown in Fig. 2. When deploying data streaming in a manufacturing shopfloor as nowadays numerous industrial control data layers are built by Ethernet communication, which accommodates the signal exchanges among PLCs, robots, distributed IOs, etc.

Processing raw point cloud data needs surface filtering and smoothing, which solved by Statistical Outlier Removal and MLS. A Voxel Grid filter can also be applied to down sample mesh points using a K-D Tree Search on a surface space. Down-sampled points are regularly distributed and hence easier to be simulated by Shape Terra. Triangular meshes also needs to be cleaned if any outlier vertex is removed. The cleaning process on meshed surfaces first remove the triangular meshes which refer to detected outliers. Then, clustering on the meshes is performed based on their connectivity, and only the biggest cluster representing the actual part shape is kept. At this point, smoothed surfaces cleaned from detectable outliers and noises is prepared for *Shape Terra* model. In cases where scanning using multiple cameras or multiple scanning poses, there are some available

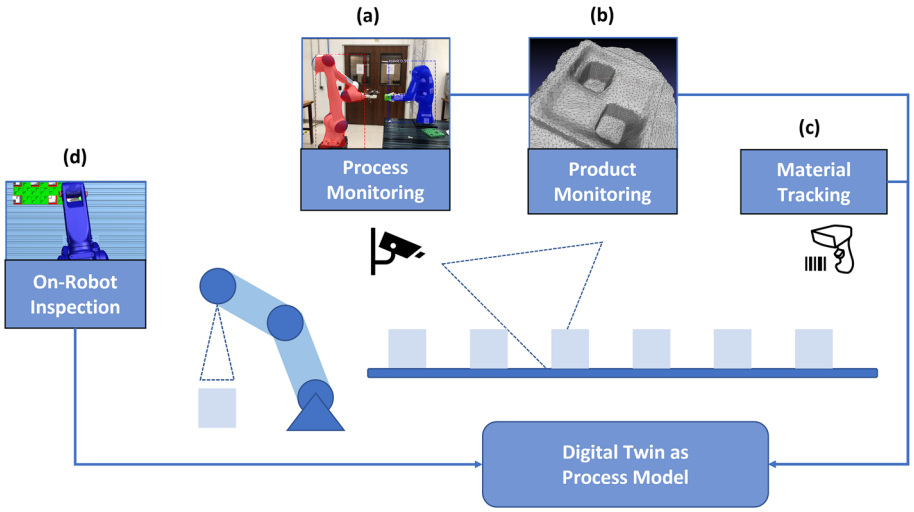

Fig. 2 Vision-aided robotic manufacturing processes automated with digital twinning: **a** process monitoring using computer vision system; **b** product state monitoring by shape retrieval; **c** material tracking and recording with bar code; **d** In-situ inspection with on-robot cameras

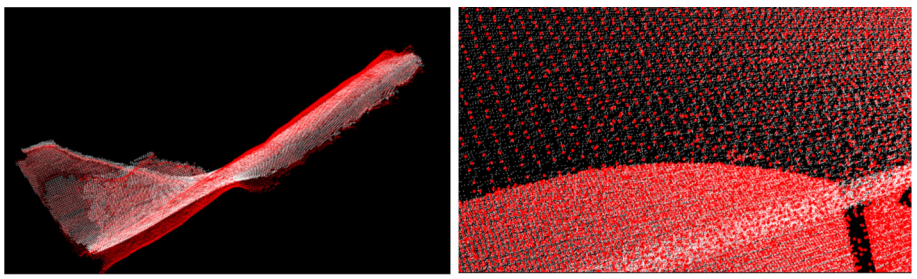

(a) **(b)**

Fig. 3 Scanned 3D surface processing using **a** Moving Least Square and **b** Voxel Grid filtering

methods for surface reconstruction, such as Poisson Surface Reconstruction (Kazhdan et al., 2006) and Ball Pivoting (Bernardini et al., 1999). 3D point cloud and 2.5D triangulation are directly retrieved from the cameras. A regulated scanning shape is shown in Fig. 3.

The *shape Terra* model

Given the rationale of HKS (Sun et al., 2009) as a heat diffusion equation caused by surface conductivity in a spatial $\mathbb{R}3$ domain shown in Eq. (1), the numerical model derived by this approach can be similarly applied to 3D mesh files assuming heat retention properties of a structure explicitly imply the Gaussian curvature of the underlined surfaces. The relationship between HKS and Gaussian curvature is defined as in Eq. (1)-(7).

$$\Delta_M u_{(x,t)} + \frac{\partial u_{(x,t)}}{\partial t} = 0 \tag{1}$$

where $u_{(x,t)}$ can be seen as the heat located at vertex x and time step t. Δ_M is the Laplace–Beltrami operator of manifold M. Therefore, the heat kernel between point x and y at time step t is defined as amount of heat transferred from x to y in time t, given a unit heat is applied at y. The heat kernel $k_t(x, y)$ from x to y is constraint by heat operator H_t that exponentiates Δ_M:

$$H_t f(x) = \int_M k_t(x, y) f(y) dy \tag{2}$$

where $H_t = e^{-t\Delta_M}$, heat operator H_t maps the initial heat distribution f to the corresponding heat distribution at time t. Thus, the heat kernel $k_t(x, y)$ satisfies Eq. (2) is correlative to the weighted average over all the heat transfer paths from x to y. It can be defined by a Gaussian function in d-dimensional Euclidean space $\mathbb{R}^{\mathrm{d}}$:

$$k_t(x, y) = (4\pi t)^{-\frac{d}{2}} e^{-\frac{||x-y||^2}{4t}} \tag{3}$$

In a general Riemannian manifold, a mesh Laplacian operator L has been used to calculate the discretized curvature on surfaces. Based on which, Mesh Laplacian operator L_c by cotangent formula (Belkin et al., 2008) generates a $n \times n$ matrix that stores the connectivity information between all the n vertices. *HKS* proposes to constrain this curvature information to a temporal domain:

$$L_c u_t = -\frac{\partial u_t}{\partial t} \tag{4}$$

This can be solved by:

$$u_t = e^{-L_c t} u_0 \tag{5}$$

If needed, Dirichlet boundary condition $u_{(x,t)} = u_{(x,0)}$ can be applied for all vertices x on the boundary of manifold M (all $x \in \partial M$) at all t.

Matrix exponential $e^{-L_c t}$ can be solved by a general eigen decomposition. L_c, as a $n \times n$ real symmetric matrix, can be decomposed by $L_c = \varnothing \mathbf{\Lambda} \varnothing^T$, where $\varnothing$ is an orthogonal matrix whose columns are the eigenvectors of L_c, and $\mathbf{\Lambda}$ is a diagonal matrix whose entries are the eigenvalues of L_c. Given the power series definition of matrix exponential, implementation of heat operator becomes:

$$e^{-L_c t} = \varnothing e^{-\mathbf{\Lambda} t} \varnothing^T A \tag{6}$$

HKS is defined to measure how much heat remains at vertex x if unit amount of heat is applied at $t = 0$:

$$k_t(x, x) = \sum_{i=0}^{\infty} e^{-\lambda_i t} \phi_i(x)^2 \tag{7}$$

ϕ_i and λ_i represent the i-th eigenvector and eigenvalue of L_c matrix at the vertices, which are stored in matrix $\varnothing$ and $\mathbf{\Lambda}$.

Surface Mesh generates six connectivity for each non-boundary vertices, hence we detect boundaries by finding all the vertices that do not satisfy this. Then, a Dirichlet (first-type) boundary condition is applied on a discretized meshes of raw surface. Namely, Dirichlet Boundary Condition specifies a fixed value of heat at manifold boundary$x \in \partial$M. Neumann Boundary Condition (second type) specifies a fixed derivative over all $x \in \partial$M, by which means alters the intrinsic geometries. Thus, feature curvatures reside at boundaries are altered. Hence, a Dirichlet Boundary Condition can be formulated as:

$$u_{(x,t)} = u_0 \text{ for } \forall x \in \partial \text{M and } \forall t \tag{8}$$

Hence there is: $\frac{\partial u_{(x,t)}}{\partial \text{t}} = 0$. Recall Eq. (5) heat $u_t = e^{-L_c t} u_0$, one can obtain:

$$L_c(x) = 0 \text{ for } \forall x \in \partial \text{M} \tag{9}$$

A unique signature, Persistent Heat Signature R_v, is generated at each vertex. Recall $k_t(x, y)$ quantifies all the heat transfer paths from a vertex y to x. Assume a vertex x records its own heat retention, which integrates all the heat transfer to y over manifold M. If there is a unit heat applied to the vertex x, which has an initial heat distribution $f(x)$. The retained heat value R_x is described as:

$$R_x(t) = f(x) - H_t f(x) = f(x) - \int_M k_t(x, y) f(y) dy \tag{10}$$

Persistent Heat Value (PHV) R_v is defined to be the integration of retained heat R_x over a designated amount of time t_m, given an initial heat distribution f. We define t_m as the time when maxima of HKS is reached since $t = 0$ when a unit heat is applied. R_v is able to compare different points on the normalized time domain.

$$R_v(x) = \int_0^{t_m} R_x(t) dt \tag{11}$$

PHV calculation on some typical mechanical features are shown in Fig. 4. with the t_i as 1000 discrete time steps with a step interval of 0.001 s. R_v generated at each point is stored for pattern recognition such as identify, differentiate, or matching salient features on the shape, which is used as a unique feature recognizer by *Shape Terra*.

The virtual thread accommodated in *Process Simulate* can detect process anomalies by simulation, such as robot reachability or objects collisions in designed paths. *Shape Terra* is further to simulate and numerically monitor inherent curvatures if any on-going structural deviation. It is envisioned to detect geometrical differences from continuous product scanning, which derives human-level knowledge by comparing signatures with corresponding CAD and scan files. By mapping Persistent Heat Signatures with pointwise intrinsic curvatures, minor geometrical differences will lead to differently distributed PHVs. Using a Laplace operator for Laplace–Beltrami operator calculation to implement this simulation, which facilitates *Shape Terra* a promising candidate to process 3D meshes.

Discretized Laplacian operator L_c is calculated as a matrix where each element at boundary vertices is constraint to be 0. As a result, we can observe a temporal HKS distribution constraint by the Dirichlet boundary condition in Fig. 5. Figure 5a–e plot the heat dissipation process given an in initial heat at the freeform surface. Figure 5f plots the heat retention value; this is referred as the PHS in this work. The detected boundaries have a constant heat value over the time and varied locations, which is the same value at the uniformly applied heat distribution when $t = 0$. The heat kernel signatures at boundary vertices remain same as the initial heat distribution, which is a unit heat applied at these locations.

Towards a product-driven digital twin system enabling rapid shape inference and adaptive process control, live product status shall be acquired by cameras or sensors. For example, shape-critical object detection for a machine visual inspection can be used by both additive and subtractive manufacturing, assuming the defect types are recognizable in

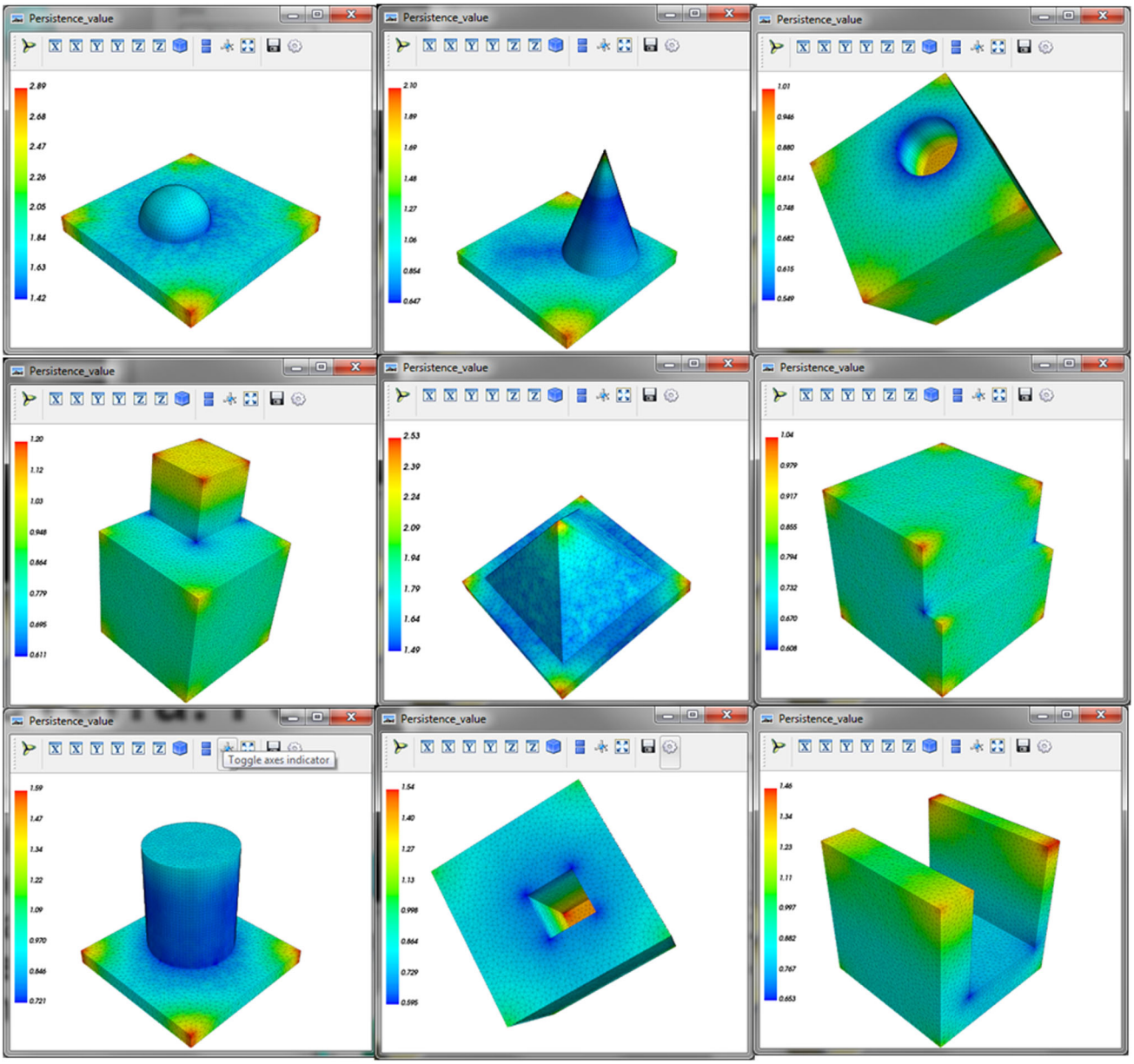

Fig. 4 *Shape Terra* calculation on 9 CAD mesh files of typical mechanical features: dome, cone, blind hole, protrusion, pyramid, step, boss, pocket, slot

detected shapes. Developing such manufacturing intelligence is explored in this work to for rapid in-process assessment using 3D scanning.

Deployment to CAE platforms and control systems

System integration of HKS-based *Shape Terra* was firstly built on a Computer-Aided Engineering (CAE) platform, Siemens *Tecnomatix Process Simulate*. The authors have been utilizing this platform for virtual commissioning, process prediction, and control verification by constructing a CAE-based digital twin aligned with physical counterparts (Xia et al., 2019, 2020). To expand the usage of such CAE-based digital twin implementation, feature extraction on shape data is further explored in this work. Shape features are extracted from the virtual environment, with vertices and mesh information stored inside CAD files. Computer aided platforms are usually composed of library with virtual object instances, object-oriented databases, and engines that perform required computing. Virtual objects defined by general accepted CAD formats, such as stl, step, and jt, can be directly accessed and used to retrieve mesh information. A *Shape Terra* Graphic User Interface (GUI) is implemented in this

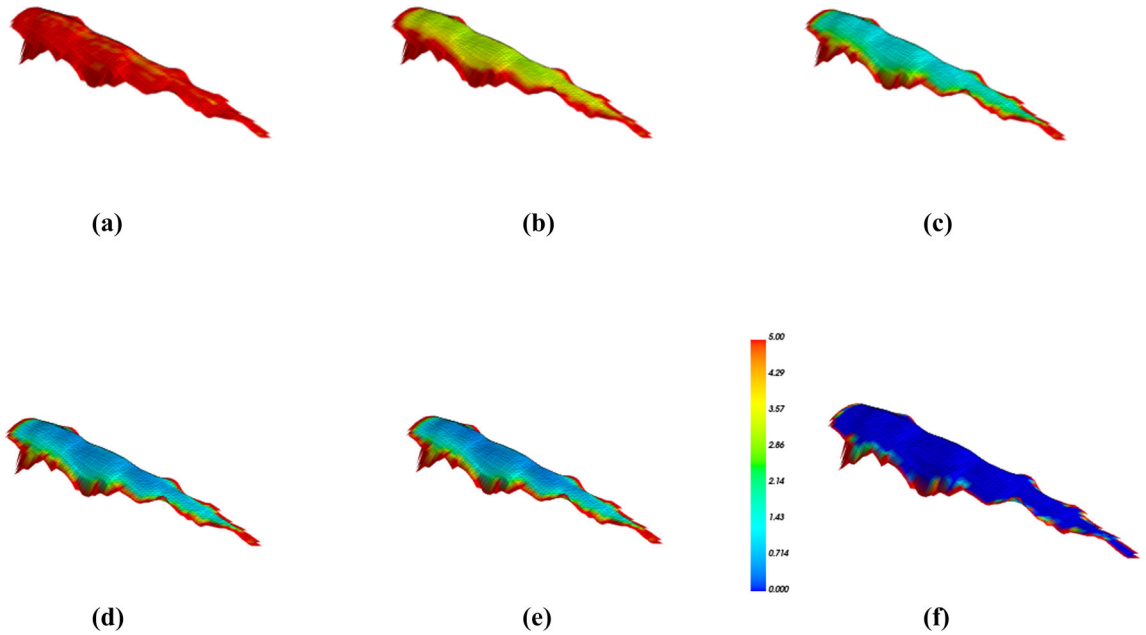

Fig. 5 Temporal HKS distribution at a partial surface scan constraint by the Dirichlet boundary condition. Subplot (**a**–**e**) present the HKS at 1st, 11th, 51st, 300th, and 800th time step. The cumulative Persistent Heat Value is shown in subplot (**f**)

work using application programming interface, which controls the defined functions and exchanges data with external platforms, see Fig. 6.

GUI designed for *Shape Terra* has three major functions: (1) connect to external environments to perform model calculations. In this work, *Shape Terra* calculations rely on large-scale eigensolvers. The user can easily perform these calculations while staying in the Process Simulate front end. (2) auto-generate large volume of shape meshes. Part features can be generated with random or user-specified locations and dimensions on a surface. This function builds large datasets to train pattern recognition algorithm using Convolutional Neural Networks (Shi et al., 2020a, 2020b). (3) calculates HKS within the simulation process. This GUI enables users can select parts and calculate to extract shape signatures in the CAE environment. Some results can be seen in Fig. 6. (4) It interacts with the CAE environment with shape information derived by *Shape Terra*. The ability of this GUI enables streaming data and combining the simulation engine with an simulated scheduler. Using this method, previous work implements reinforcement learning agent (Xia et al., 2020) to train the autonomy of robots. Coupled with *Shape Terra*, higher resolution of such control agent tailored for manufacturing features can be trained by an intelligent computer-aided process planning application, namely a digital engine (Xia et al., 2019).

Integrating *Shape Terra* with Computer-Aided interactive platforms enables a high-resolution process planning application. In a CAE-based environment, in-situ shape manufacturability analysis can be performed by an interaction with *Shape Terra* engine. Queried part shape is retrieved from back-end database and as an input to the *Shape Terra* algorithm. Then, extracted geometrical features along with its location information can be used for the robots to plan the assembly process, e.g. which surface to grip or where to place the parts. An example process planning on a virtual fuselage assembly line is shown in Fig. 7. This software deployment of *Shape Terra* enhances the virtual counterpart of physical processes.

Intelligence integration from simulation, models, or other digital solutions into a physical manufacturing control system can be achieved by Software-in-the-loop or Hardware-in-the-loop (Lee & Park, 2014). To register detected surface feature and its PHS as machine-readable signals within the PLC control loop, this work utilized a machine-to-machine communication for industrial automation, Open Platform Communication Unified Architecture (OPC UA). The system architecture and implementation of Software-in-the-loop and Hardware-in-the-loop simulations were presented in (Xia et al., 2020). Shape knowledges are connected as a client to a OPC UA server, which stores all the process control signals. Meanwhile, deploying *Shape Terra* further generates another signal pathway from CAE environment and process virtual commissioning, where virtual features can be mapped with. Hence, registered signals can be subscribed and accessed by physical PLC (Hardware-in-the-loop), virtual PLC (Software-in-the-loop) and OPC clients (simulations, models, and digital solutions). With such system infrastructure (Fig. 8) established, the physical and virtual PLC (PLCSIM) are both able to automate the manufacturing

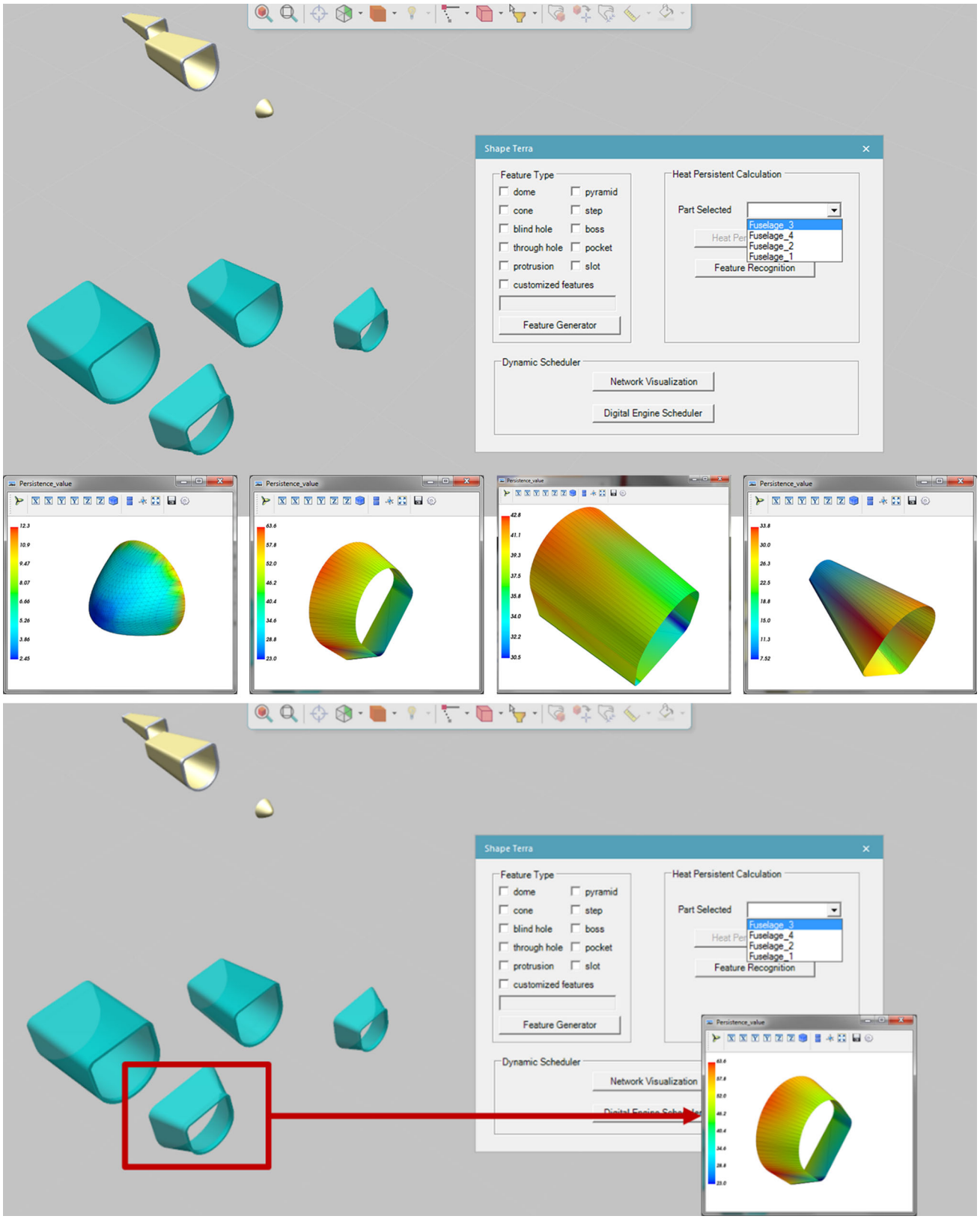

Fig. 6 An interactive GUI for *Shape Terra* hosted by Siemens Tecnomatix Process Simulate. Users select CAD using navigation tools to acquire desired shape files from the backend database for manufacturability analysis

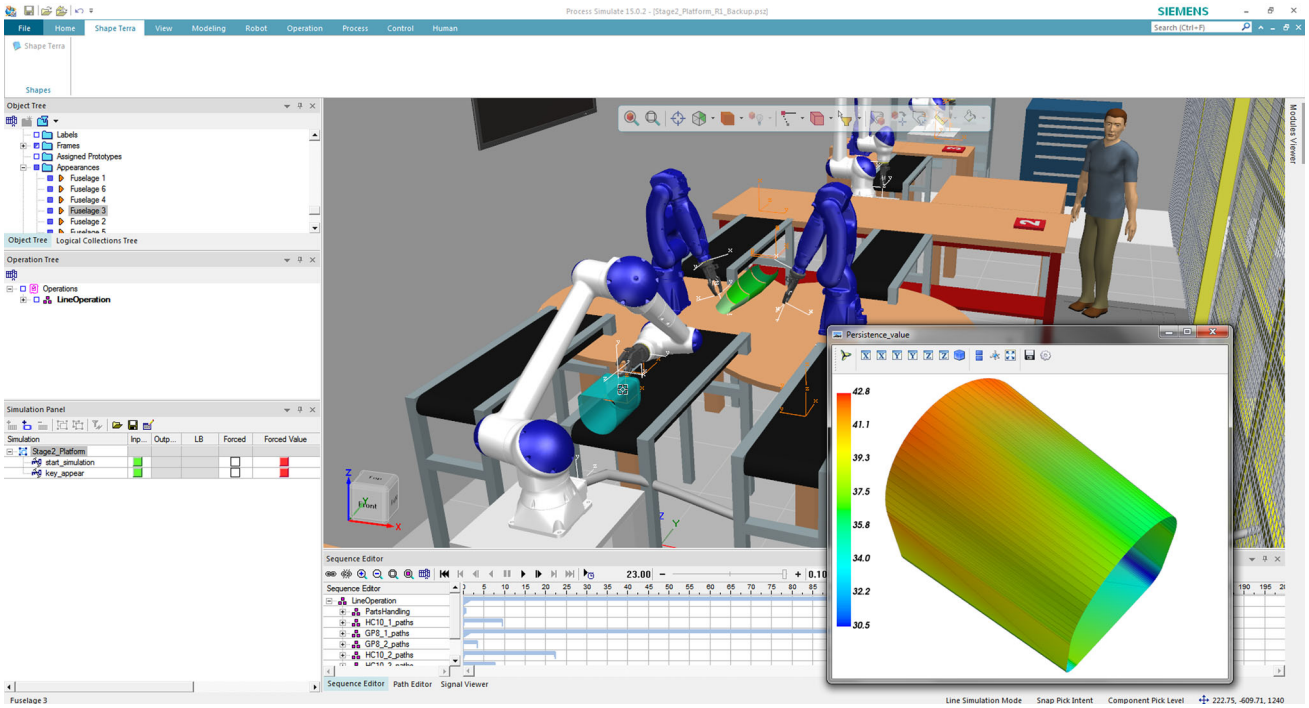

Fig. 7 Software deployment of *Shape Terra* to a Computer-Aided Process Planning (CAPP) application

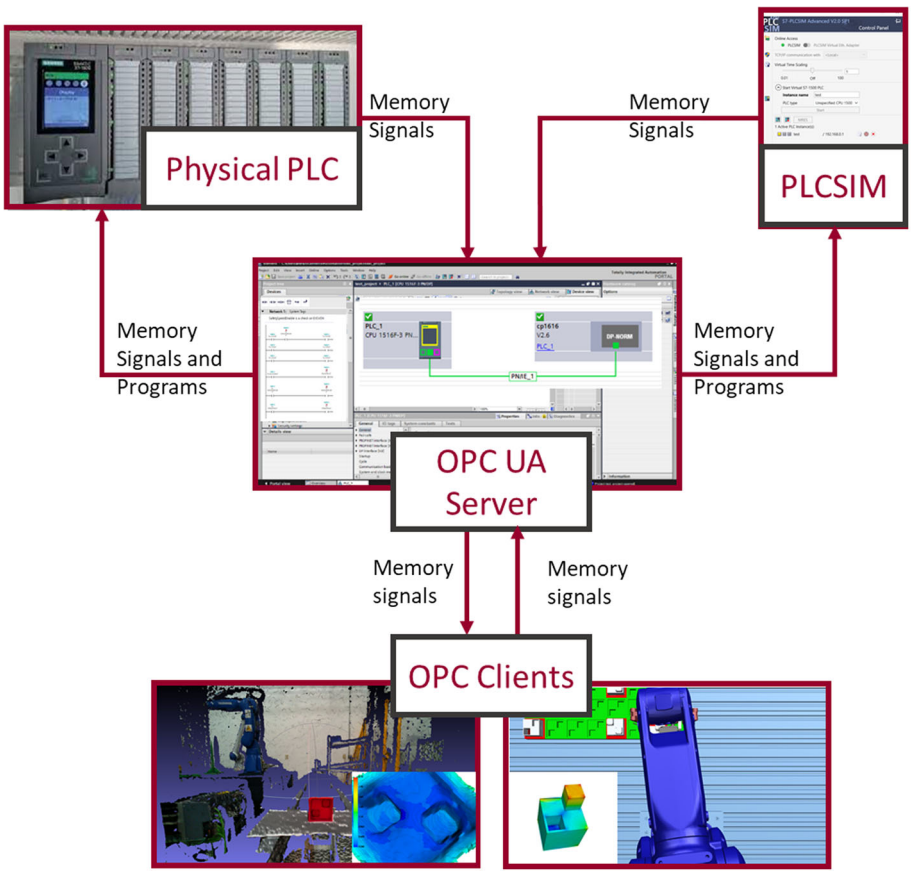

Fig. 8 A system model enabled by OPC UA machine to machine communication protocol and digital twin of Shape Terra, 3D scanning, and virtual commissioning

actions based on digital solutions such as *Shape Terra, PS,* and other platforms. Real-time semantic knowledges such as the product manufacturable features extracted from the surfaces can be explicitly translated by a similarity search in an established database. Moreover, in-situ process information such as tool center, gripping point location, can be communicated by manufacturing feature knowledges. Similarity search does not require a large-scale database to detect feature knowledges. CAD files from a simulation environment can also provide comparable values to feature signatures. Therefore, knowledge taxonomy can be accomplished by querying scanned signatures with established signatures.

Results and discussion

In this section, we present our shape signatures acquired from 3D scans for Computer-Aided Engineering (CAE) applications using the methods and materials above. First, we use multiscale filtering and clustering to extract feature clusters based on Persistent Heat Signatures (PHS). Second, a scoring function is introduced to map the shapes with tolerance of noise and irregularity. Third, signature mapping is performed on a dataset level to compare between shape files.

Multiscale filtering and feature clustering

An observation made in Fig. 9 is that PHS method is robust with different mesh triangulations and resolutions. PHS for both raw meshes and regulated meshes have similar distribution, due to the property of its intrinsic curvatures. This enables us to compare PHS in different scales and meshing methods. Since PHS calculation are expensive; one should have the option to down-sample large mesh files while preserving salient features in the mean time.

We then cluster the meshes using Persistent Heat Values (PHVs) similarities among connected vertices. On a manifold, positive Gaussian curvatures lead to larger HKS. Thus, by varying similarities, vertices can be classified by clustering into different neighbourhoods, which hint the composition of protrusion, corners, or holes. Using a clustering method, one can also filter out the unwanted boundaries in HKS matrixes. It can be observed in Fig. 10., as reducing similarities from 0.9, 0.8, to 0.75, less clusters are found, and hence cluster regions can be narrowed down for further signature extraction. In particular, Fig. 10c, f show that at a similarity of 0.9, there are isolated mesh clusters with local minima and maxima PHVs can be identified respectively as freeform and salient features to hint the existence of manufacturable features. By which means, some manufacturable feature regions extracted by *Shape Terra* are presented in Fig. 11.

Feature engineering

Extracted feature regions are further treated as shape file semantics. To compare heterogenous shape files, feature engineering will be essential to automate the process. Based on extracted features, spectral clustering is first experimented by inspecting a pool of 42 shape scans. In Fig. 12, feature distances by $\|f_1 - f_2\|_1$ and $\|\frac{1}{f_1} - \frac{1}{f_2}\|_1$ are experimented to compare the shape scan files. Figure 12. left using $\|f_1 - f_2\|_1$ demonstrates clustering results while Fig. 12 left using $\|\frac{1}{f_1} - \frac{1}{f_2}\|_1$ demonstrates discriminative results between salient features, as the first 28 files are composed with different salient features, such as protrusions, holes, steps, and edges. The last 14 files include free-form and curved surfaces.

The distance function d between two manifolds F_1 and F_2 is determined by the features f_1 and f_2, extracted by the according PHV maxima and minima. Hence for each surface scan file, we define PHS as comparable feature cluster regions f representing the maxima and minima PHV clusters. Note that minima and maxima PHV clusters caused by noise from varied scanning quality or surface boundaries can be extracted as features.

Feature vector distance function is calculated to enable signature matching between shape files. This stage consists of two steps: (1) Feature vector extraction from HPV clusters; (2) Shape matching by feature vector scoring with a predefined distance function. We build the shape dataset based on scanned shape files of products with variable geometrical characteristics. Despite the filters and multi-scale clustering applied to denoise the surfaces, there are edges and boundaries interfering with salient feature recognition results. When identifying features, there are outliers both at the boundaries and among the surfaces are identified as PHV maxima and minima along with salient features. These are respectively caused by the irregular boundaries and scanning noises on surfaces. Hence, we propose a scoring function to estimate the distance between shape features that is also robust to these outstanding challenges. To compare the feature groups between two files with the consideration of these occasions, a cross-comparison (Dey et al., 2010) is adopted to match two shapes by summarizing their closest feature distances between $\forall f_1 \in F_1$ and $\forall f_2 \in F_2$, as in Eq. (12). We performed feature engineering on selected PHV beforehand instead of directly subtract them to down-weight the comparison of outliers from noises and surface boundaries, which are simulated to surpass a value k. Meanwhile, the distances of salient features, whose PHV are expected to be smaller than k, can be compared with larger weight. It is observed that in scanned files, $k = 1$ can be pre-set for capturing most salient features. Instead of the scoring function in (Dey et al., 2010), we use inversed cluster PHV values to measure the distance between shapes:

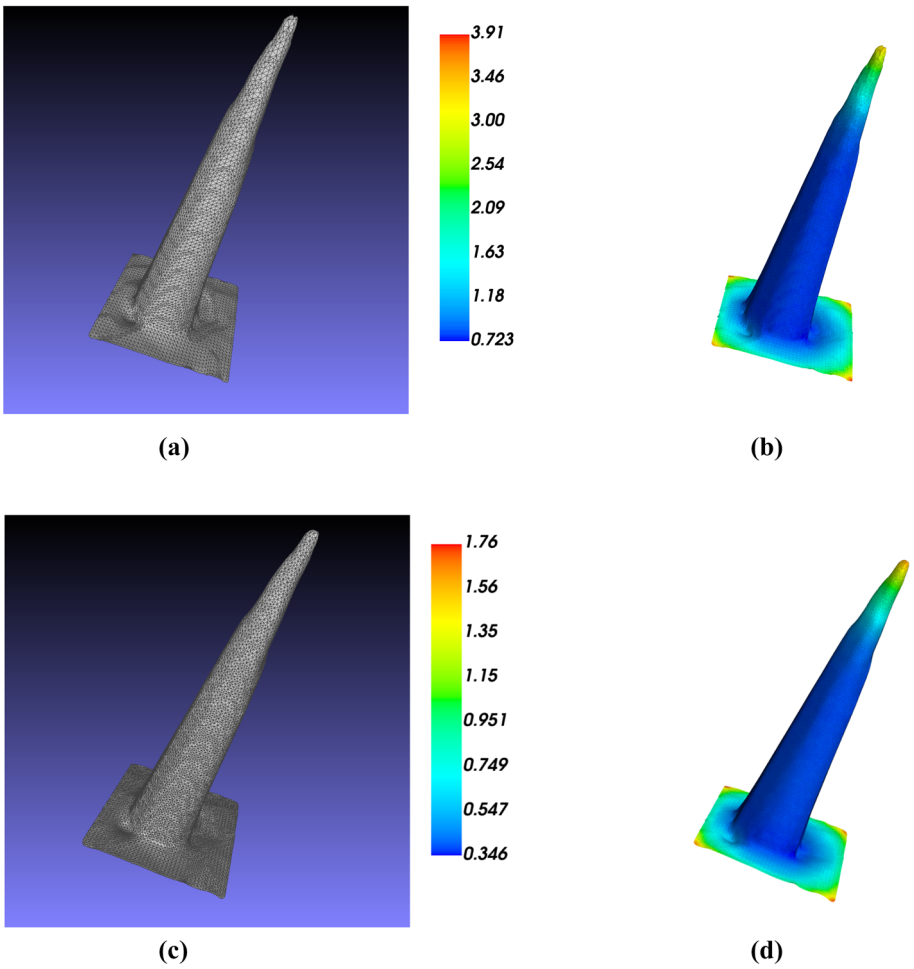

Fig. 9 PHS value distribution in **b** and **d** remain same from different meshing methods in **a** and **c**: same scan meshed by 5783 vertices and 11,393 triangular faces in **a**, **b**; and 11,982 vertices and 23,730 triangular faces 299 k triangular faces in **c**, **d**

$$d_{(F_1,F_2)} = d_{(F_2,F_1)} = \sum_{f_1 \in F_1} \min_{f_2 \in F_2} \| {f_1}^{-\frac{1}{k}} - {f_2}^{-\frac{1}{k}} \|_1 + \sum_{f_2 \in F_2} \min_{f_1 \in F_1} \left\| {f_1}^{-\frac{1}{k}} - {f_2}^{-\frac{1}{k}} \right\|_1 \quad (12)$$

Expanding the signature pool, a PHS histogram of 613 feature clusters in 76 different shape scans is shown in Fig. 13. A grid search of k is performed before an ideal feature transformation factor $k = 3$ is identified, which approximates the pool to a normal distribution. Using feature transformation, shapes files can be clustered by PHV of their signatures from salient features, free-form surfaces, surface edges or tips. When comparing shapes in a big dataset with a large volume of features, by implementing a statistical weighting, selectively compares shape files by up-weighting features with less occurrence (more unique features) in the dataset. Therefore, these features can be encoded as binary or textual codes to facilitate an interactive search engine among the signature pool. At a database level, Term Frequency Inverse-Document Frequency (TF-IDF) is used to autonomously weigh the importance of signatures by comparing their occurrence across the established dataset, which will be introduced in the following section.

Signature mapping

From Fig. 14, surface mapping results are shown by comparing similarity of extracted feature vectors $\{f_1, f_2, \ldots f_n\}$. The left figures are the query shape files with extracted signatures, and the right figures are the output shapes with the most similarities to the query files, which are measured by the least distance $d_{(F_1,F_2)}$. Despite the scan noise, query by similarities can generate robust results to compare shapes with different scanning qualities. This due to the pose-oblivious nature of heat-based signatures and noise treatment by the clustering and scoring function.

Therefore, a signatures-based search engine can be established by cross-comparison over selected features. Figure 15 shows the query results of the most similar shape files (middle and right, sorted by similarities) when inputting the original shape file (left). The matching is conducted across extracted salient features, freeform surfaces, and signature counts.

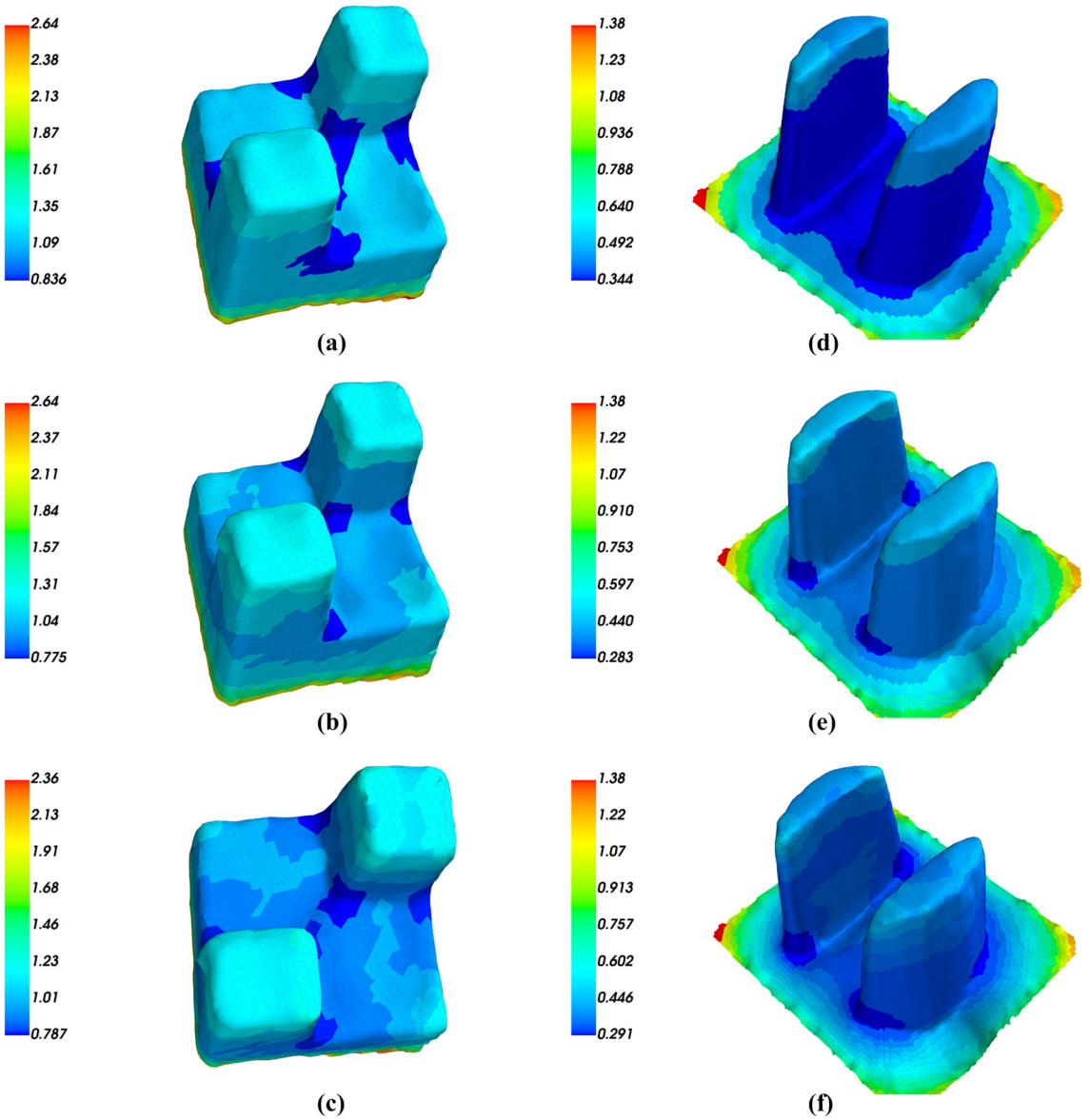

Fig. 10 PHV clustering of two shape files (left and right) by neighbourhood similarities of 0.75 in **a**, **d**, 0.8 in **b**, **e**, 0.9 in **c**, **f**

To autonomously weigh the importance of signatures, this work calculates the Term Frequency Inverse-Document Frequency (TF-IDF) for each signature by comparing its occurrence across a given shape dataset. TF-IDF is a currently approach to text-based recommender systems in Natural Languages Processing problems by quantifying importance of texts in a corpus (Beel et al., 2016), here we utilize the same approach for shape file signatures as syntaxes. Using transformed HPV as numerical inputs to TF-IDF equation (Eq. 13), one can filter out the less unique signatures and compare scanned shape files by most unique features.

$$W_{i,j} = tf_{i,j} \times \log(\frac{N}{df_i}) \tag{13}$$

where $tf_{i,j}$ is the number of occurrences of signature i in shape file j. df_i is number of shape files containing signature i. N is the total number of shape files in the signature pool. Using TF-IDF, the uniqueness of signature i can be easily quantified by its occurrence in the established signature pool. And we can autonomously extract most comparable features to semantically describe shape files. For each shape file F, an automated selection of the subset in shape file feature vector $\{f_0, f_1, f_2, \ldots f_n\}$ is accomplished and compared with other shape files by extracting the identical subsets. The feature vectors superset consist of normalized signature counts f_0 and signature values $\{f_1, f_2, \ldots f_n\}$. The results are presented in Fig. 16.

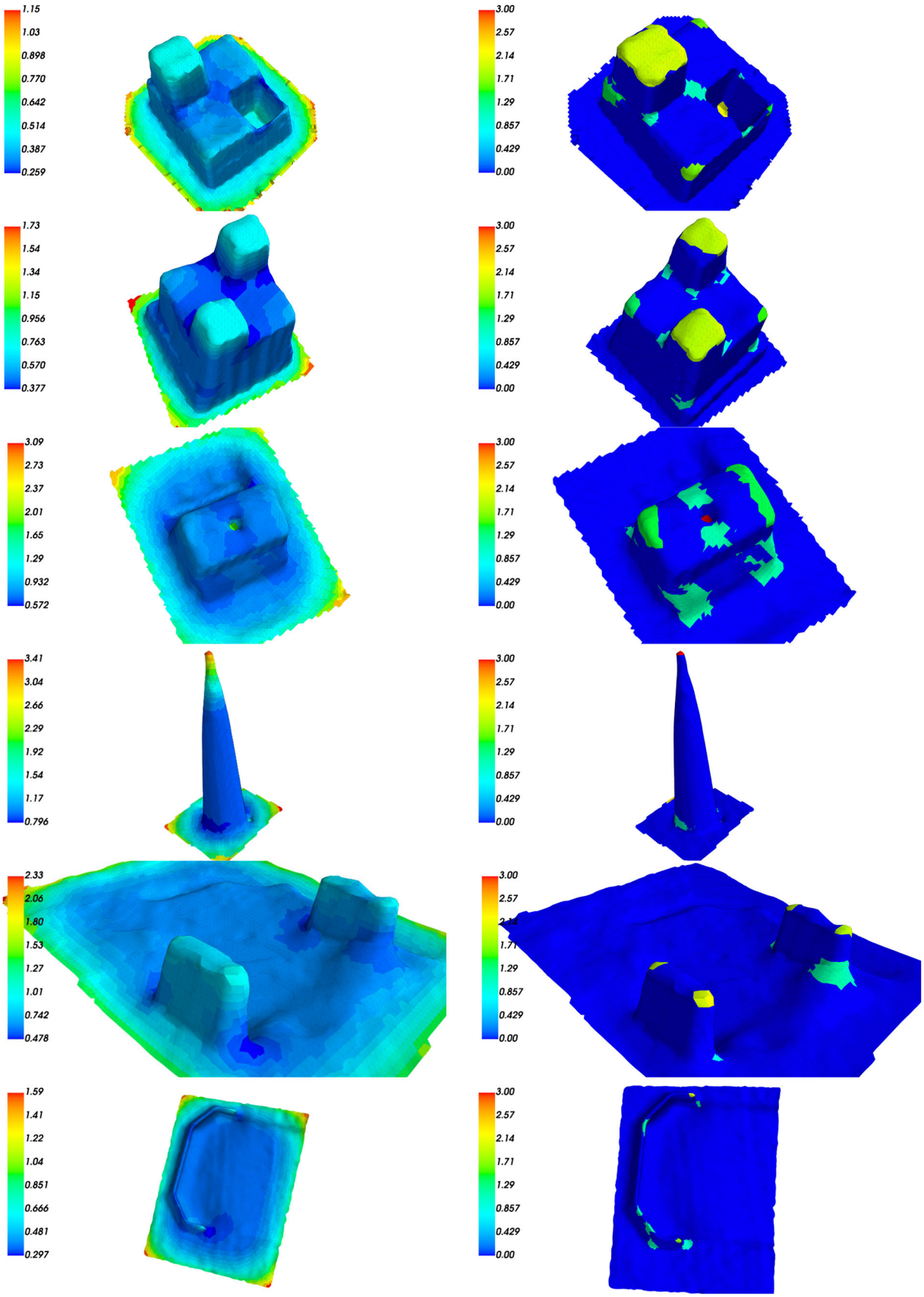

Fig. 11 Persistent Heat Signatures (PHS) extraction as manufacturable features (right) using maxima and minima PHV clusters (left) by a neighbourhood similarity of 0.9

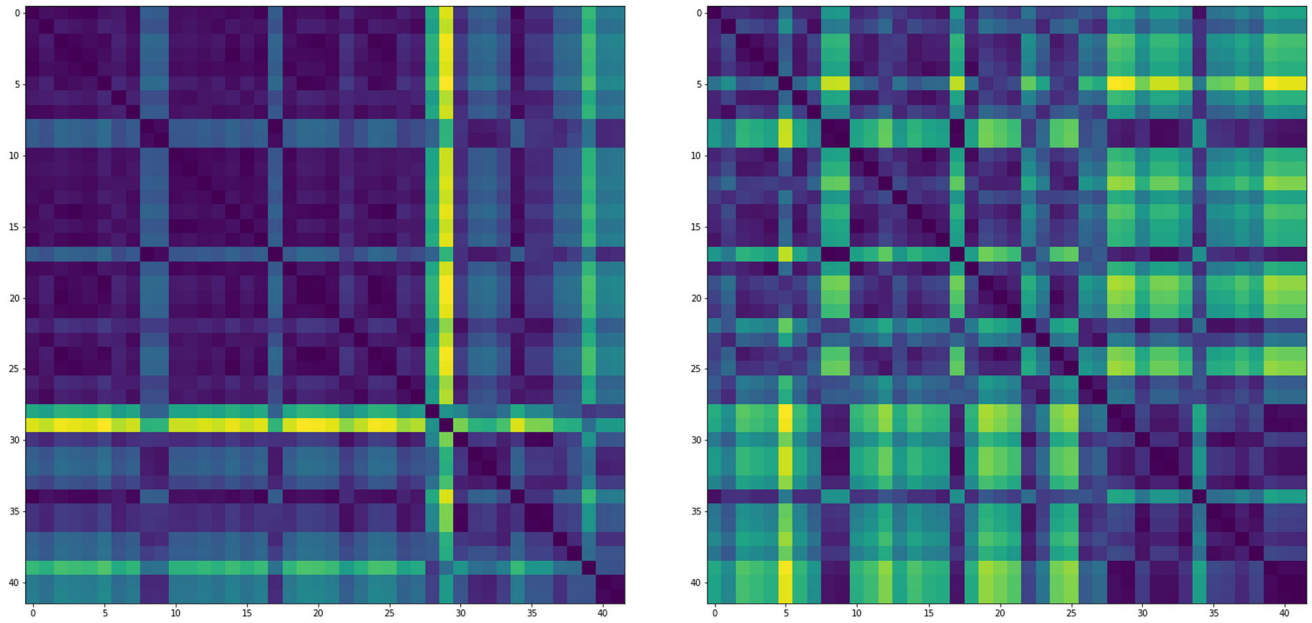

Fig. 12 Spectral clustering of 42 shape files on Persistent Heat Signatures by feature transformation functions (left: $\|f_1 - f_2\|_1$; right: $\|\frac{1}{f_1} - \frac{1}{f_2}\|_1$)

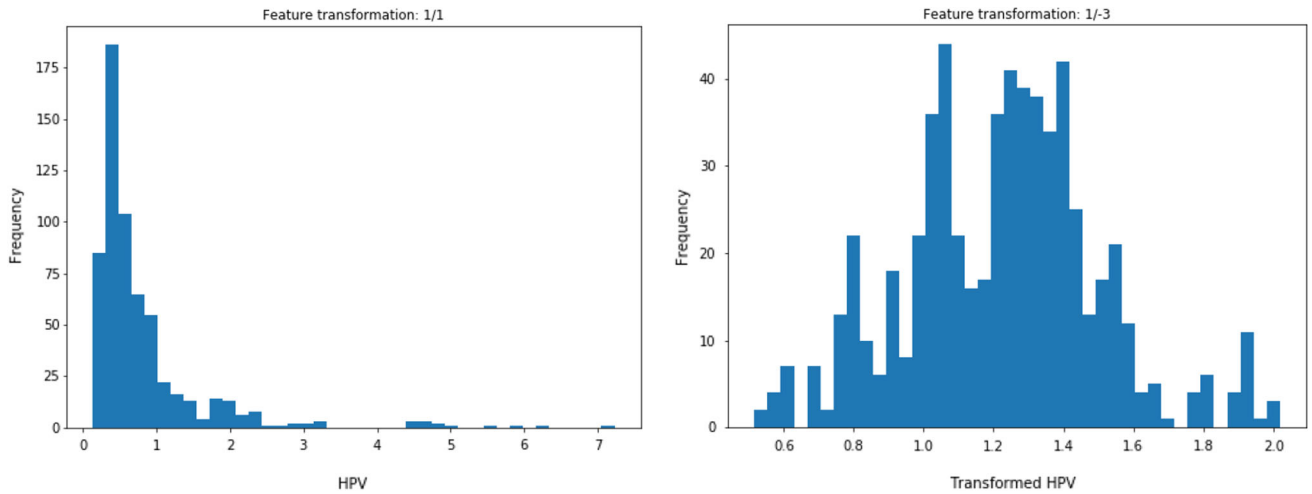

Fig. 13 Histograms of PHS pool (Left: original PHS f; Right: transformed PHS by $f^{-\frac{1}{k}}$ with $k = 3$)

Conclusion and outlook

This work aims to address challenges posted towards cognitive digital twinning featuring in-situ shape-critical manufacturing intelligence. It is enabled by the system-level automation of geometrical and topological learning for product features. A product-centered Digital Twin implementation is described focusing on the following contributions:

(1) Data (D): Heat-based signatures, traditionally applied to extract semantics from CAD meshes, are calculated in this work to take a novel signature-based approach to intrinsic knowledges from runtime product data stream. This adds extra values to legacy production process data by automating manufacturing feature extraction and utilizing frame-wise visual scenes.

(2) Model(M): Increasing shape data utilization by identifying unique manufacturing features and comparing extracted signatures. Point-wise signatures propose a high-resolution method to facilitate semantic segmentation on raw meshes. The proposed semantic extraction reduces local information loss from all mesh connectivity stored over high-dimensional manifolds. Meanwhile, mapping heat-based signatures reduces dependency on scan device positioning and input mesh styles, given the pose-oblivious and shape-critical signatures generated by *Shape Terra*. In addition, such simulative methods

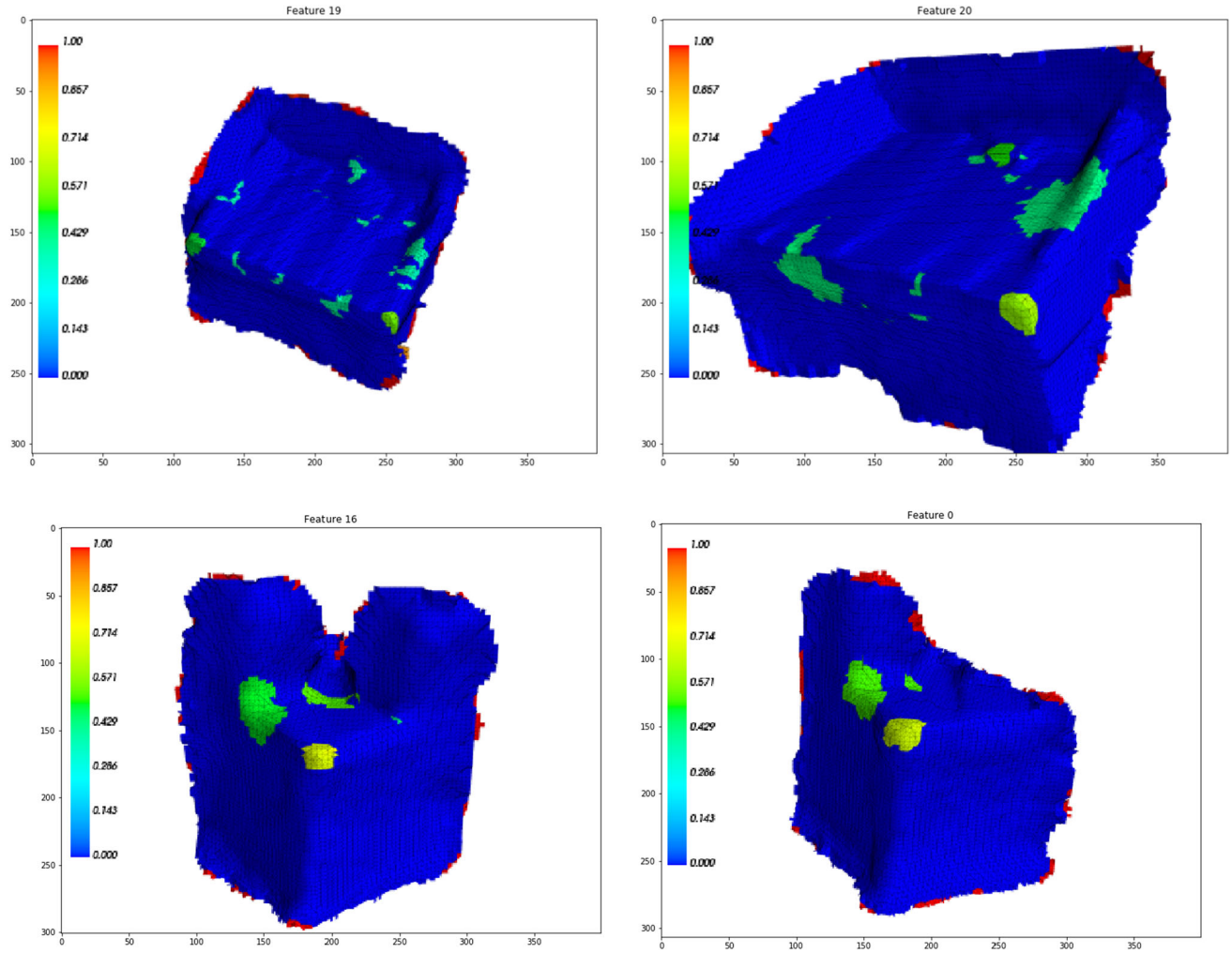

Fig. 14 Feature vectors mapping: (left) shape files highlighting extracted feature clusters; (right) output shapes with the most similarities to the query files

can generate knowledge without requiring voluminous, quality, and balanced training data.

(3) Service(S): Contributing in-situ structural sensing to Human–Machine interoperable manufacturing automation enabled by feature-level information system. A novel smart manufacturing system built on point-wise, pose-oblivious signatures reduces human supervision for in-situ product quality assessment, which leads to highly autonomous visual monitoring for surface forming and material handling processes. Human interoperable communication with functions of shape selection, query, and knowledge search in historical signature pool that can be built on top of the extracted semantic layer.

As a result, the proposed research creates a novel digital twin implementation featuring geometrical modelling and signature searching during shape-forming productions. It is intended to timely detect human-level knowledges of process risks such as structural variations, which might be unavailable to practitioners immediately in many manufacturing scenarios. Heat Kernel-based approach increases the understanding of information residing in investigated product structures, as well as its potential influences by thermal and mechanical behaviours. Structural predictions can be made and continuously modelled following empirical methodologies with a variety of what-if analysis, which facilitates a highly automated control of product conditions.

In future work, a 3D scanned manufacturing feature query system will be established towards a highly automated robotic shape retrieval mechanism and hence to enable human–machine interoperable decision-makings such as in robotic inspection. Shape signature pool has only limited volumes in this work, reflecting the expensiveness of manufacturing process data. This limitation is also common when deriving data-driven manufacturing intelligence

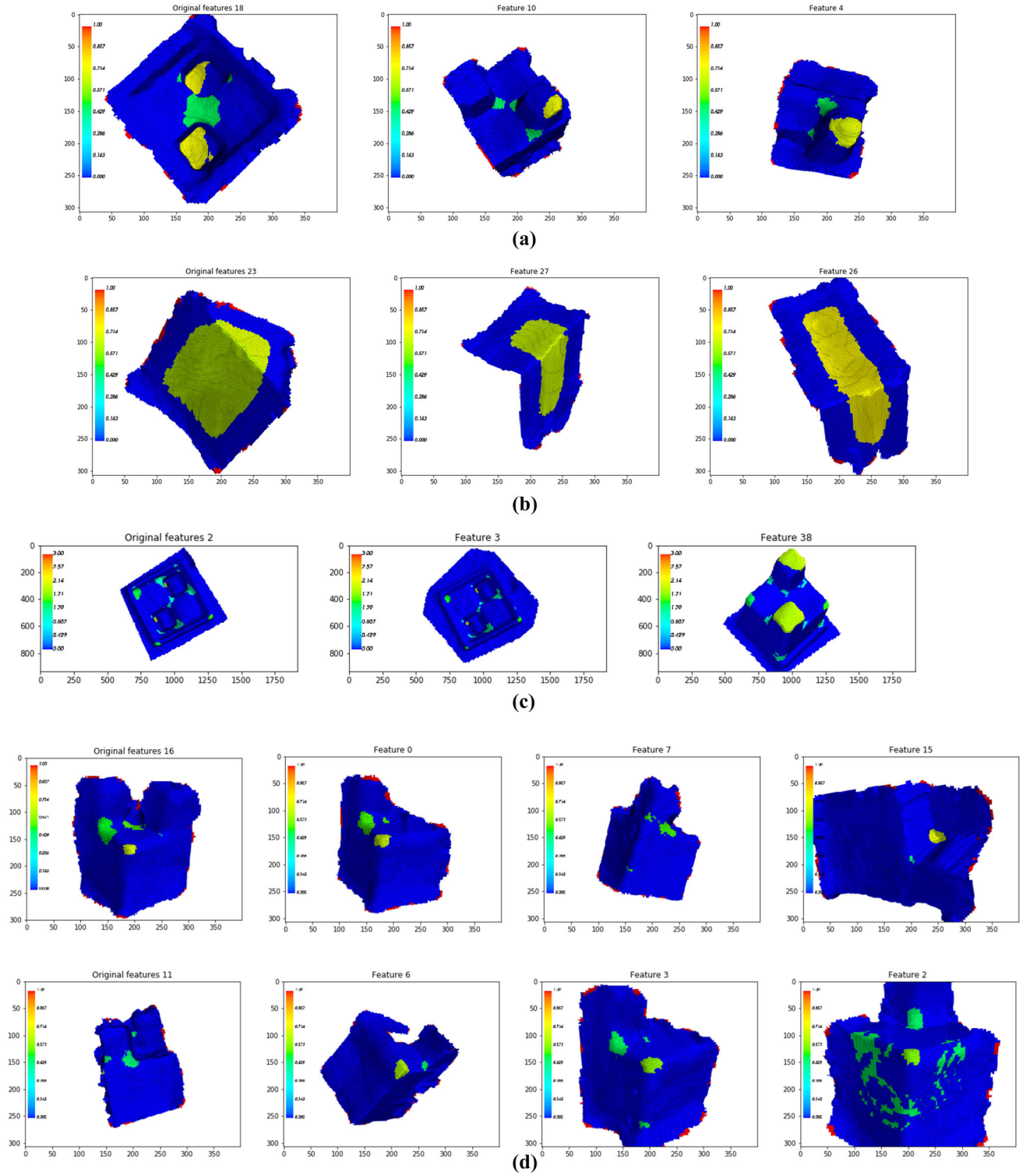

Fig. 15 A shape file search engine with input original features (left) and output most similar feature lists (the remaining features sorted by their similarity): **a** mapping by salient features (local maximas); **b** mapping on freeform surfaces (local minima); **c** mapping by signature counts; **d** mapping across multiple salient feature vectors $\{f_1, f_2, \ldots f_n\}$

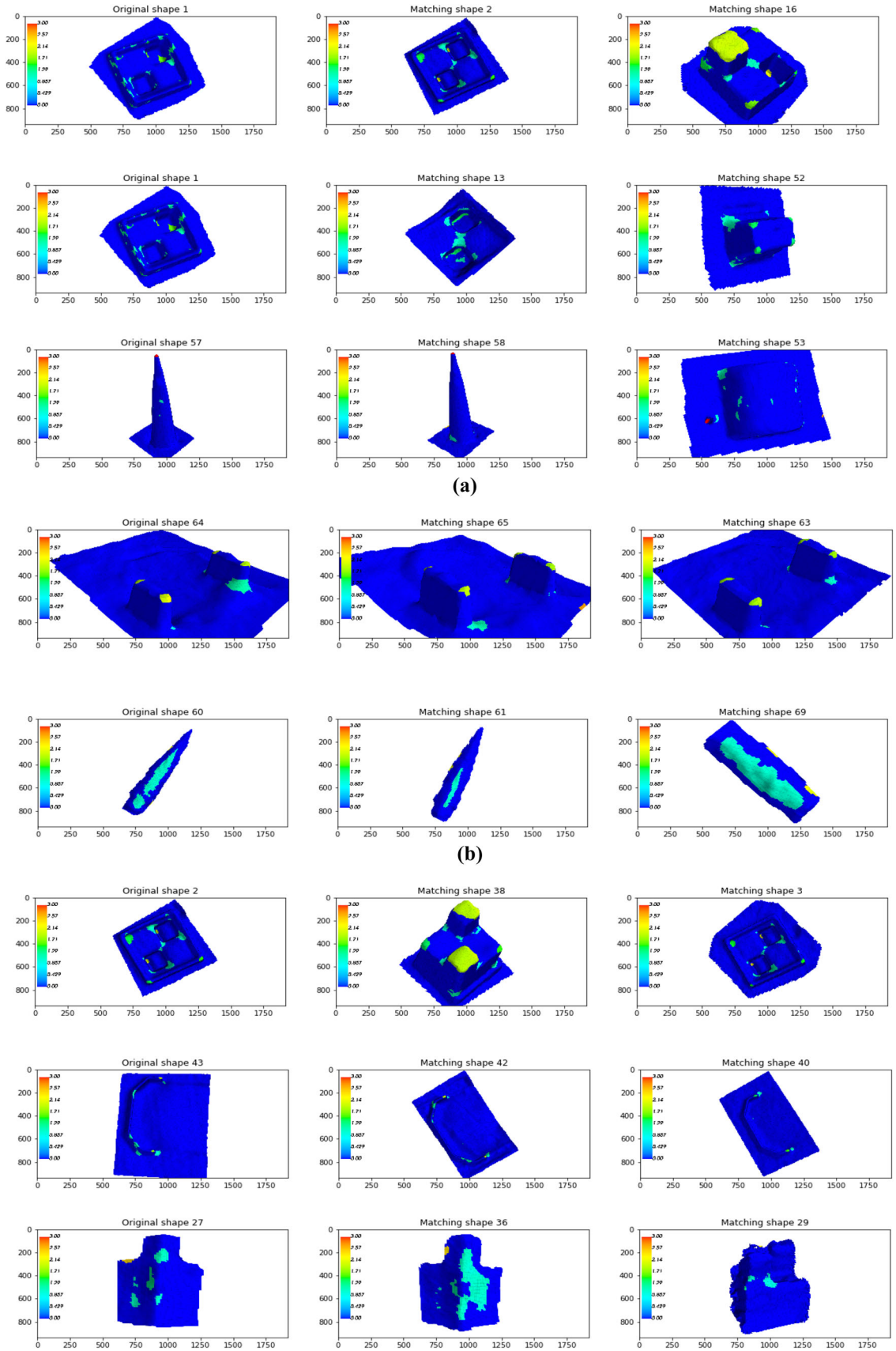

Fig. 16 Shape file matching by selection criteria over TF-IDF values of feature vector $\{f_0, f_1, f_2, \ldots f_n\}$: **a** $\{f_1, f_2, \ldots f_n\}$ only; **b** $\{f_0\}$ only; **c** $\{f_1, f_2, \ldots f_n\}$ and $\{f_0\}$

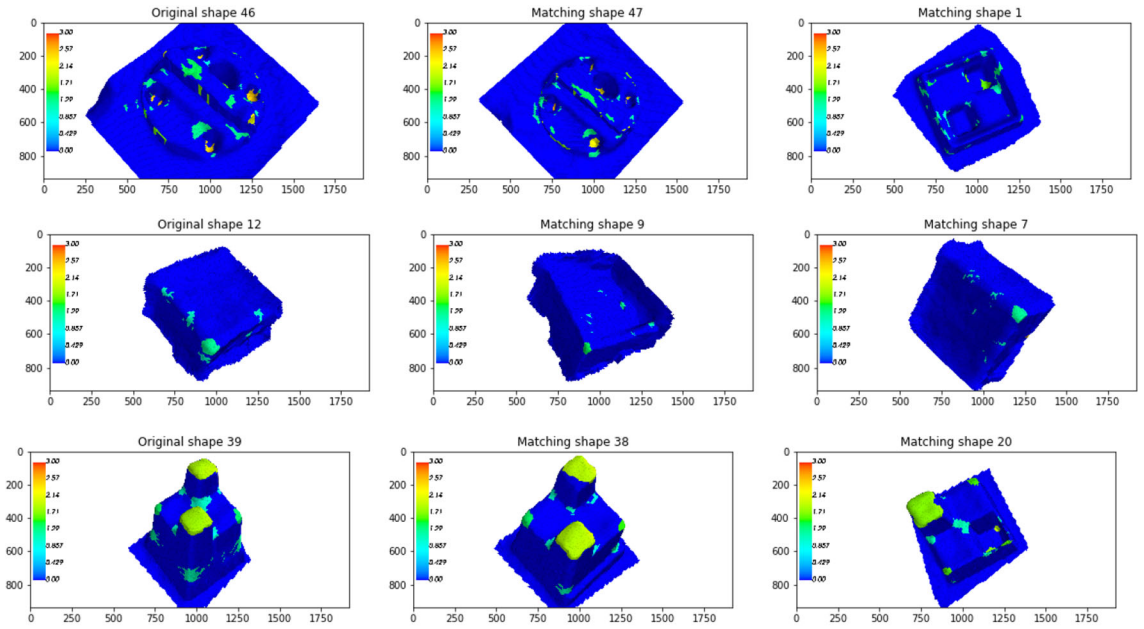

(c)

Fig. 16 continued

using machine learning models, which shows the advantages of simulative models such as *Shape Terra*. Compared with machine learning approaches, proposed model is less affected by the abundance and the quality of datasets. We perform simple distance clustering over a small sample of PHS to obtain semantic significance from scanned shapes, while similar feature extraction on 3D data by machine learning often require training large neural networks. Less dependency on data abundance provides our approach more applicability to industrial manufacturing use cases. Future emphasis will be put on a hybrid approaches to the human knowledges of shape data by utilizing data-driven learning systems. By developing a large dataset and intelligent manufacturing shape knowledge query system, we will seek to overcome the limitations and establish a platform for real-world structural knowledge reuse and shape annotation. Registered structural images, CAD models, heat-based signatures and other data will be stored and reused as domain assets for rapid manufacturing feature mapping.

Acknowledgements This material is based upon work supported by the National Science Foundation under Grant No. 2119654 and the South Carolina Research Authority. Any opinions, findings, and conclusions or recommendations expressed in this material are those of the author(s) and do not necessarily reflect the views of the National Science Foundation or the South Carolina Research Authority.

Funding Funding was provided by South Carolina Research Authority (10009353, 10009367) and National Science Foundation (2119654).

References

Adamson, G., Wang, L., & Moore, P. (2017). Feature-based control and information framework for adaptive and distributed manufacturing in cyber physical systems. *Journal of Manufacturing Systems, 43*, 305–315.

Bai, X., Wilson, R., & Hancock, E. (2005). Characterising Graphs using the Heat Kernel. In *British machine vision conference 2005*. Retrieved from https://academic.microsoft.com/paper/1966071755

Bao, J., Guo, D., Li, J., & Zhang, J. (2019). The modelling and operations for the digital twin in the context of manufacturing. *Enterprise Information Systems, 13*(4), 534–556.

Beel, J., Gipp, B., Langer, S., & Breitinger, C. (2016). Research-paper recommender systems: A literature survey. *International Journal on Digital Libraries, 17*(4), 305–338.

Belkin, M., Sun, J., & Wang, Y. (2008). Discrete laplace operator on meshed surfaces. In *Proceedings of the twenty-fourth annual symposium on Computational geometry*, (pp. 278–287). Retrieved from https://academic.microsoft.com/paper/2097824281

Bernardini, F., Mittleman, J., Rushmeier, H., Silva, C., & Taubin, G. (1999). The ball-pivoting algorithm for surface reconstruction. *IEEE Transactions on Visualization and Computer Graphics, 5*(4), 349–359.

Bronstein, A., Bronstein, M., Guibas, L., & Ovsjanikov, M. (2011). Shape google: Geometric words and expressions for invariant shape retrieval. *ACM Transactions on Graphics, 30*(1), 1–20.

Bronstein, M., & Kokkinos, I. (2010). Scale-invariant heat kernel signatures for non-rigid shape recognition. In *2010 IEEE computer society conference on computer vision and pattern recognition*, (pp. 1704–1711). Retrieved from https://academic.microsoft.com/paper/2007206727

Cai, N., Bendjebla, S., Lavernhe, S., Mehdi-Souzani, C., & Anwer, N. (2018). Freeform machining feature recognition with manufacturability analysis. *Procedia CIRP, 72*, 1475–1480.

Charles, R., Su, H., Kaichun, M., & Guibas, L. (2017). PointNet: deep learning on point sets for 3D classification and segmentation. In

2017 IEEE conference on computer vision and pattern recognition (CVPR), (pp. 77–85). Retrieved from https://academic.microsoft.com/paper/2560609797

Davtalab, O., Kazemian, A., Yuan, X., & Khoshnevis, B. (2020). Automated inspection in robotic additive manufacturing using deep learning for layer deformation detection. *Journal of Intelligent Manufacturing*, 1–14. Retrieved from https://academic.microsoft.com/paper/3092226864

Denkena, B., Henning, H., & Lorenzen, L.-E. (2010). Genetics and intelligence: New approaches in production engineering. *Production Engineering, 4*(1), 65–73.

Dey, T., Li, K., Luo, C., Ranjan, P., Safa, I., & Wang, Y. (2010). Persistent heat signature for pose-oblivious matching of incomplete models. *Computer Graphics Forum, 29*(5), 1545–1554.

Dong, J., & Vijayan, S. (1997). Features extraction with the consideration of manufacturing processes. *International Journal of Production Research, 35*(8), 2135–2155.

Ebel, H., Riedelsheimer, T., & Stark, R. (2021). Enabling automated engineering's project progress measurement by using data flow models and digital twins. *International Journal of Engineering Business Management*. Retrieved from https://academic.microsoft.com/paper/3198913245

ElGhawalby, H., & Hancock, E. (2015). Heat kernel embeddings, differential geometry and graph structure. *Axioms, 4*(3), 275–293.

Geng, W., Chen, Z., He, K., & Wu, Y. (2016). Feature recognition and volume generation of uncut regions for electrical discharge machining. *Advances in Engineering Software, 91*, 51–62.

Harik, R., Shi, Y., & Baek, S. (2017). Shape Terra: Mechanical feature recognition based on a persistent heat signature. *Computer-Aided Design and Applications, 14*(2), 206–218.

Huang, W., Mei, X., Jiang, G., Hou, D., Bi, Y., & Wang, Y. (2021). An on-machine tool path generation method based on hybrid and local point cloud registration for laser deburring of ceramic cores. *Journal of Intelligent Manufacturing*, 1–16.

Jiang, Z., Guo, Y., & Wang, Z. (2021). Digital twin to improve the virtual-real integration of industrial IoT. *Journal of Industrial Information Integration, 22*, 100196.

Jones, P., Maggioni, M., & Schul, R. (2008). Manifold parametrizations by eigenfunctions of the Laplacian and heat kernels. *Proceedings of the National Academy of Sciences of the United States of America, 105*(6), 1803–1808.

Kazhdan, M., Bolitho, M., & Hoppe, H. (2006). Poisson surface reconstruction. In *Proceedings of the fourth Eurographics symposium on Geometry processing*, (pp. 61–70). Retrieved from https://academic.microsoft.com/paper/2008073424

Kokkinos, I., & Yuille, A. (2008). Scale invariance without scale selection. In *2008 IEEE conference on computer vision and pattern recognition*, (pp. 1–8). Retrieved from https://academic.microsoft.com/paper/2148261123

Lai, Z.-H., Tao, W., Leu, M., & Yin, Z. (2020). Smart augmented reality instructional system for mechanical assembly towards worker-centered intelligent manufacturing. *Journal of Manufacturing Systems, 55*, 69–81.

Lee, C., & Park, S. (2014). Survey on the virtual commissioning of manufacturing systems. *Journal of Computational Design and Engineering, 1*(3), 213–222.

Li, J., Zhou, Q., Huang, X., Li, M., & Cao, L. (2021). In situ quality inspection with layer-wise visual images based on deep transfer learning during selective laser melting. *Journal of Intelligent Manufacturing*, 1–15.

Liu, X., Li, Y., Ma, S., & Lee, C.-H. (2015). A tool path generation method for freeform surface machining by introducing the tensor property of machining strip width. *Computer-Aided Design, 66*, 1–13.

Marchetta, M., & Forradellas, R. (2010). An artificial intelligence planning approach to manufacturing feature recognition. *Computer-Aided Design, 42*(3), 248–256.

Monostori, L., Kádár, B., Bauernhansl, T., Kondoh, S., Kumara, S., Reinhart, G., Sauer, O., Schuh, G., Sihn, W., & Ueda, K. (2016). Cyber-physical systems in manufacturing. *Cirp Annals-Manufacturing Technology, 65*(2), 621–641.

Mortlock, T., Muthirayan, D., Yu, S.-Y., Khargonekar, P., & Faruque, M. (2021). Graph learning for cognitive digital twins in manufacturing systems. arXiv:2109.08632.

Newcombe, R.A., Izadi, S., Hilliges, O., Molyneaux, D., Kim, D., Davison, A.J., Kohi, P., Shotton, J., Hodges, S., & Fitzgibbon, A. (2011). KinectFusion: Real-time dense surface mapping and tracking. In *2011 10th IEEE international symposium on mixed and augmented reality*, (pp. 127–136). Retrieved from https://academic.microsoft.com/paper/1987648924

Nie, W., Zhao, Y., Liu, A.-A., Gao, Z., & Su, Y. (2020). Multi-graph Convolutional Network for Unsupervised 3D Shape Retrieval. In *Proceedings of the 28th ACM international conference on multimedia*, (pp. 3395–3403). Retrieved from https://academic.microsoft.com/paper/3092933617

Nonaka, Y., Erdős, G., Kis, T., Kovács, A., Monostori, L., Nakano, T., & Váncza, J. (2013). Generating alternative process plans for complex parts. *Cirp Annals-Manufacturing Technology, 62*(1), 453–458.

Nonaka, Y., Erdős, G., Kis, T., Nakano, T., & Váncza, J. (2012). Scheduling with alternative routings in CNC workshops. *Cirp Annals-Manufacturing Technology, 61*(1), 449–454.

Park, Y., Woo, J., & Choi, S. (2020). A cloud-based digital twin manufacturing system based on an interoperable data schema for smart manufacturing. *International Journal of Computer Integrated Manufacturing, 33*(12), 1259–1276.

Pokojski, J., Szustakiewicz, K., Woźnicki, Ł, Oleksiński, K., & Pruszyński, J. (2021). Industrial application of knowledge-based engineering in commercial CAD/CAE systems. *Journal of Industrial Information Integration, 25*, 100255.

Rameshbabu, V., & Shunmugam, M. (2009). Hybrid feature recognition method for setup planning from STEP AP-203. *Robotics and Computer-Integrated Manufacturing, 25*(2), 393–408.

Redelinghuys, A., Basson, A., & Kruger, K. (2020). A six-layer architecture for the digital twin: A manufacturing case study implementation. *Journal of Intelligent Manufacturing, 31*(6), 1383–1402.

Saidy, C., Xia, K., Sacco, C., Kirkpatrick, M., Kircaliali, A., Nguyen, L., & Harik, R. (2020). Building future factories: a smart robotic assembly platform using virtual commissioning, data analytics, and accelerated computing. *SAMPE.*

Schleich, B., Anwer, N., Mathieu, L., & Wartzack, S. (2017). Shaping the digital twin for design and production engineering. *Cirp Annals-Manufacturing Technology, 66*(1), 141–144.

Shi, Y., Zhang, Y., Baek, S., Backer, W., & Harik, R. (2018). Manufacturability analysis for additive manufacturing using a novel feature recognition technique. *Computer-Aided Design and Applications, 15*(6), 941–952.

Shi, Y., Zhang, Y., & Harik, R. (2020a). Manufacturing feature recognition with a 2D convolutional neural network. *Cirp Journal of Manufacturing Science and Technology, 30*, 36–57.

Shi, Y., Zhang, Y., Xia, K., & Harik, R. (2020b). A Critical Review of Feature Recognition Techniques. *Computer-Aided Design and Applications, 17*(5), 861–899.

Sun, J., Ovsjanikov, M., & Guibas, L. (2009). A concise and provably informative multi-scale signature based on heat diffusion. In *SGP '09 Proceedings of the Symposium on Geometry Processing* (Vol. 28, pp. 1383–1392).

Sundararajan, V., & Wright, P. (2004). Volumetric feature recognition for machining components with freeform surfaces. *Computer-Aided Design, 36*(1), 11–25.

Sunil, V., & Pande, S. (2008). Automatic recognition of features from freeform surface CAD models. *Computer-Aided Design, 40*(4), 502–517.

Tao, F., Qi, Q., Wang, L., & Nee, A. (2019). Digital twins and cyber-physical systems toward smart manufacturing and industry 4.0: correlation and comparison. *Engineering, 5*(4), 653–661.

Vaxman, A., Ben-Chen, M., & Gotsman, C. (2010). A multi-resolution approach to heat kernels on discrete surfaces. *International Conference on Computer Graphics and Interactive Techniques, 29*(4), 121.

Wells, L., Dastoorian, R., & Camelio, J. (2021). A novel NURBS surface approach to statistically monitor manufacturing processes with point cloud data. *Journal of Intelligent Manufacturing, 32*(2), 329–345.

Wells, L., Megahed, F., Niziolek, C., Camelio, J., & Woodall, W. (2013). Statistical process monitoring approach for high-density point clouds. *Journal of Intelligent Manufacturing, 24*(6), 1267–1279.

Xia, K., Sacco, C., Kirkpatrick, M., Harik, R., & Bayoumi, A.-M. (2019). Virtual Comissioning of Manufacturing System Intelligent Control. *SAMPE 2019 - Charlotte, NC*. Retrieved from https://academic.microsoft.com/paper/2939160706

Xia, K., Sacco, C., Kirkpatrick, M., Saidy, C., Nguyen, L., Kircaliali, A., & Harik, R. (2020). A digital twin to train deep reinforcement learning agent for smart manufacturing plants: Environment, interfaces and intelligence. *Journal of Manufacturing Systems., 58*, 210–230.

Xia, K., Saidy, C., Kirkpatrick, M., Anumbe, N., Sheth, A., & Harik, R. (2021a). Towards semantic integration of machine vision systems to aid manufacturing event understanding. *Sensors, 21*(13), 4276.

Xia, T., Zhang, W., Chiu, W., & Jing, C. (2021b). Using cloud computing integrated architecture to improve delivery committed rate in smart manufacturing. *Enterprise Information Systems, 15*(9), 1260–1279.

Yli-Ojanperä, M., Sierla, S., Papakonstantinou, N., & Vyatkin, V. (2019). Adapting an agile manufacturing concept to the reference architecture model industry 4.0: A survey and case study. *Journal of Industrial Information Integration, 15*, 147–160.

Zhang, X., & Ming, X. (2020). Reference subsystems for Smart Manufacturing Collaborative System (SMCS) from multi-processes, multi-intersections and multi-operators. *Enterprise Information Systems, 14*(3), 282–307.

Zhang, X., Nassehi, A., & Newman, S. (2014). Feature recognition from CNC part programs for milling operations. *The International Journal of Advanced Manufacturing Technology, 70*(1), 397–412.

Zhang, X., Tsang, W.-M., Yamazaki, K., & Mori, M. (2013). A study on automatic on-machine inspection system for 3D modeling and measurement of cutting tools. *Journal of Intelligent Manufacturing, 24*(1), 71–86.

Zhang, X., Zheng, Y., Suresh, V., Wang, S., Li, Q., Li, B., & Qin, H. (2020). Correlation approach for quality assurance of additive manufactured parts based on optical metrology. *Journal of Manufacturing Processes, 53*, 310–317.

Zhao, C., Du, S., Lv, J., Deng, Y., & Li, G. (2021). A novel parallel classification network for classifying three-dimensional surface with point cloud data. *Journal of Intelligent Manufacturing*, 1–13

Zhou, Y., & Tuzel, O. (2018). VoxelNet: End-to-end learning for point cloud based 3D object detection. In *2018 IEEE/CVF conference on computer vision and pattern recognition*, (pp. 4490–4499). Retrieved from https://academic.microsoft.com/paper/2963727135